Imaging Cycling Tumor Hypoxia

Shingo Matsumoto, Hironobu Yasui, James B. Mitchell, and Murali C. Krishna

Abstract

Cycling hypoxia is now a well-recognized phenomenon in animal and human solid tumors. Cycling hypoxia can exist more than 100-μm distances from a microvessel, and some of these regions have been shown to exist adjacent to normal tissue. Fluctuations in pO_2 of approximately 20 mm Hg can occur with periodicities of minutes to hours and even days. These fluctuations have been attributed to changes in erythrocyte flux, perfusion, and also development of newer vascular networks. Cycling hypoxia has been shown to induce the expression of hypoxia-inducible transcription factor-1α (HIF-1α) and also confer tumor cells and tumor vascular endothelial cells with enhanced prosurvival pathways, making tumors less responsive to radiation and chemotherapy. Imaging of cycling hypoxia in tumors can provide capabilities to help plan appropriate treatment, by taking into account the magnitude and frequency of fluctuations and also their locations adjacent to normal tissue. Electron paramagnetic resonance imaging (EPRI) provides the ability to distinguish chronic and cycling hypoxic regions and has the required spatial and temporal resolutions to provide quantitative maps of tumor pO_2. EPRI can serve as a valuable tool in examining tumor pO_2 longitudinally in response to treatment and in an experimentally chosen time window to spatially map fluctuations in pO_2 noninvasively in animal models of implanted or orthotopic tumors, with a potential for human applications. *Cancer Res; 70(24); 10019–23. ©2010 AACR.*

Background

Hypoxia in solid tumors, caused by an imbalance in oxygen supply and demand, can be responsible for resistance to radiotherapy and chemotherapy (1). Tumor hypoxia is generally attributed to chaotic and poorly organized vasculature (2, 3). On the basis of histologic assessment, the presence of hypoxia in human tumors and its role in treatment resistance were postulated by Thomlinson and Gray (4), and this was verified in rodent tumors (5) and later in humans as well (6). Although chronic hypoxia, which exists in regions of tumors beyond the diffusion distance of oxygen, is well known, more recently, acute hypoxia or intermittent hypoxia, now known as cycling hypoxia, is receiving increased attention because of the significant influence on treatment resistance displayed by both tumor cells as well as the endothelial cells of tumor vasculature (7, 8).

Cycling hypoxia and its relevance in tumor radiobiology and/or radioresistance were studied several decades ago in animal models (9, 10). Chaplin and colleagues investigated the temporal profile of tumor oxygenation and found that cycling hypoxia resulted from transient fluctuations in tumor perfu-

sion (11). This phenomenon was investigated in more detail, and it was found to be correlated with fluctuations in erythrocyte flux, which in turn were attributed to factors including transient occlusion of vasculature and narrowing of vasculature (2, 12). Subsequent studies showed that the fluctuations were not exclusively adjacent to blood vessels but could even occur as far as 130 μm from a microvessel (13). The observation that at least 20% of tumor cells experience cycling hypoxia in SCCVII tumors (11) supports the notion that cycling hypoxia is a common feature in solid tumors and can be considered a hallmark in tumor microcirculation (2, 14).

Frequency of Cycling

The frequency of cycling hypoxia has been studied in several model systems using a variety of techniques (2). Research from these studies suggests that, whereas cycling is ubiquitous in xenografts, orthotopic solid tumors, and in human tumors, the cycling frequency can range between a few cycles per minute to hours or even days (2, 14). Although the higher frequency cycling hypoxia has been associated with several factors, including changes in perfusion, erythrocyte flux, and vascular occlusion, among others, cycling hypoxia observed over a period of days has been attributed to changes in vascular network structures as a consequence of neoangiogenesis (2, 14).

Consequences of Cycling Hypoxia

One consequence of cycling hypoxia is increased metastatic potential of cells in tumors, experiencing periods of acute hypoxia followed by reoxygenation. The mechanisms

Authors' Affiliation: Radiation Biology Branch, Center for Cancer Research, National Cancer Institute, Bethesda, Maryland

Corresponding Author: Murali C. Krishna, Radiation Biology Branch, Center for Cancer Research, National Cancer Institute, Building 10, Room B3B69, NIH, 9000 Rockville Pike, Bethesda, MD 20892-1002. Phone: 301-496-7511; Fax: 301-480-2238. E-mail: murali@helix.nih.gov

underlying this phenomenon are associated with phenotypic changes induced in the primary tumor cells (15). The cellular effects of cycling hypoxia were investigated by Moeller and colleagues in tumor and endothelial cells subjected to periods of hypoxia followed by periods of reoxygenation (16). They found that reoxygenation postradiation in tumor cells resulted in a significant increase in reactive oxygen species (ROS) accompanied by stabilization of HIF-1α, even under aerobic conditions (16). Further, it was found that postradiation reoxygenation increased vascular endothelial growth factor levels and conferred resistance to endothelial cells against radiation damage (7, 8). These effects were inhibited by administration of antioxidant enzyme mimics, suggesting a strong role for ROS in the observed responses at a cellular level (16). When the role of HIF-1α in radiation response was investigated in more detail, it was found that HIF-1α can be involved in radiosensitization of tumor cells and can even cause radioresistance by stimulating endothelial cell survival pathways dependent on treatment sequencing (17). A recent study examining the effects of experimentally imposed cycles of hypoxia, followed by reoxygenation on endothelial cells, found them to be resistant to radiation and also increased their ability to migrate and assemble into microvessels (8). This resistant phenotype was found to be accompanied by accumulation of HIF-1α during periods of induced hypoxia. Similar experiments in tumor-bearing mice, which, when subjected to cycles of breathing gas containing high (21%) and low (7%) oxygen, resulted in lower levels of radiation-induced apoptotic death in both endothelial and tumor cells as well as increased rate of tumor regrowth (8).

Tumor Hypoxia and HIF-1α

Intratumoral hypoxia causes increased expression and activity of HIF-1α, which plays a pivotal role in tumor progression, angiogenesis, metabolic switch to aerobic glycolysis, metastasis, and resistance to treatment (14). HIF-1α overexpression, now associated with poor clinical outcome, has been shown in experimental animal models to have marked effects on tumor growth, making it an important target for inhibition in cancer therapy (18). Exposure to ionizing radiation upregulates HIF-1α activity in tumors, which eventually results in tumor radioresistance through vascular radioprotection mediated by ROS-supported processes, making it an important target for radiosensitization (16). It was found that sequencing of HIF-1α inhibition and radiation therapy are important in treatment outcome (17). These observations point to the role for noninvasive and serial examination of tumor oxygenation status and fluctuations in tumor oxygen during an observation window to design an effective treatment sequence with radiation and HIF-1α inhibition.

A major question is how cycling hypoxia contributes to the complicated relationship between HIF-1, hypoxia, and patient prognosis. Martinive and colleagues have recently reported that endothelial cells exposed to experimental cycling hypoxia exhibit more robust accumulation of HIF-1α than cells that are chronically hypoxic (8). Endothelial cells subjected to experimental cycling hypoxia acquire proangiogenic phenotypes and resistance to apoptotic treatment, which seems to be mediated by HIF-1α, because HIF-1α–small interfering (si)RNA abrogated the phenotypes induced by cycling hypoxia. Similar robust accumulation of HIF-1α signals by experimentally enforced cycling hypoxia has been reported in mouse carotid body and isolated perfused heart models (2, 14). It is noteworthy that cycling hypoxia–induced robust accumulation of HIF-1α can be observed only in hypoxic periods but not in interrupting reoxygenation periods because of its rapid degradation (8); whereas enhanced expression of HIF-1α–regulating genes are observed even in the reoxygenation periods. Collectively, cycling hypoxia in tumors has greater potential to promote HIF-1α stabilization and overexpression of HIF-1α–regulating proteins even in regions proximal to vascular wall (within oxygen diffusion distance) than in chronically hypoxic regions. This process turns on a proangiogenic switch and contributes to survival of endothelial cells and their feeding tumor cells against cytotoxic treatments. Further research is needed to study the effects of spontaneous cycling hypoxia on HIF-1α accumulation in tumor cells and surrounding supporting cells.

Imaging Cycling Hypoxia

Although the phenomenon of cycling hypoxia was originally observed as a consequence in *in vivo* radiobiological experiments followed by *in vitro* assessment, the work of Chaplin and colleagues obtained strong experimental evidence that directly established the occurrence of this phenomenon in animal models (11). Subsequent window-chamber experiments provided insights into the mechanisms underlying this phenomenon and also established the temporal profile and the spatial extent from blood vessels in which this phenomenon occurs (2, 12). Because *a priori* information on cycling tumor hypoxia may be useful in planning radiotherapy and chemotherapy regimens, imaging techniques are being explored actively to monitor this phenomenon with the required spatial and temporal resolutions.

The original noninvasive studies of cycling hypoxia employed the window-chamber model and obtained experimental data that helped gain valuable insights into the phenomena and also the mechanisms responsible for cycling hypoxia (2). Subsequent efforts concentrated in using clinically available imaging modalities to study these phenomena. Baudelet and colleagues were the first to successfully show cycling hypoxia using magnetic resonance imaging (MRI)–based approaches, such as T_2^*-weighted MRI and dynamic contrast enhanced (DCE)-MRI in animal models to monitor temporal changes in tumor oxygenation (19). In this study, they noticed two kinds of regions in tumor with respect to time-dependent changes in pO_2. Regions with typical up-and-down fluctuations in T_2^* indicative of cycling hypoxia were noted along with a pattern of steadily decreasing pO_2 in other regions. These studies validated the existence of cycling hypoxia in tumors using imaging methods that can, in principle, be conducted in humans. However, as pointed out in that report, the contributions of other factors involved in the determination of oxygenation made the widespread use of these MRI-based

approaches not optimal. Using phosphorescence-life time imaging, Cardenas-Navia and colleagues examined three different rat tumors models and detected the occurrence of cycling hypoxia in all three models, with characteristic periodicities pointing to the general feature of cycling hypoxia (13). Additionally, in two tumor types, they found spatio-temporal correlations of fluctuations within the tumor (13).

To use the wealth of information generated from animal studies, it is important to develop imaging strategies that can monitor cycling hypoxia, preferably quantitatively, in animals and humans. Optical-based imaging techniques, although valuable in well-defined animal model systems and helpful to the development of deeper insights into cycling hypoxia biology, may have limitations in penetration depth, preventing the studies of larger animal or human tumors. Positron emission tomography (PET) was the first imaging technique applied to study cycling hypoxia in humans (20). Although it is possible to use PET imaging to map tumor hypoxia using nitroimidazole drugs such as ^{18}F-misonidazole, this approach only provides an integrating assessment of hypoxia in a predetermined time window after the drug is administered; it cannot monitor cycling hypoxia unless the frequency of cycling hypoxia is over a period of several days. The situation is similar when using immunohistochemistry to assess hypoxia in *ex vivo* analyses of tumor tissues after excision from tumor-bearing animals injected with pimonidazole (21). A desirable technique for imaging hypoxia would be noninvasive; quantitative in pO_2 measurements; repeatable over minutes, hours and days; able to coregister with anatomic images; and, in principle, scaled for human applications.

Key Advances

Dynamic three-dimensional electron paramagnetic resonance imaging (EPRI) and its capability of noninvasively visualizing spontaneous cycling hypoxia in murine tumor models have been recently described (22). EPRI is a low field magnetic resonance technique similar to nuclear magnetic resonance. The collisional interaction between molecular oxygen, which is paramagnetic, and an exogenously administrated paramagnetic tracer broadens the EPR line width of the tracer, thus rendering a quantitative estimate of tissue oxygen concentration. Although noninvasive hypoxia-imaging techniques already use clinically available modalities such as MRI, PET, and optical imaging, EPRI has several unique advantages: (1) it is noninvasive and measures pO_2 deep in tissue without radioisotopes, (2) it provides absolute pO_2 values with resolution of 3 to 4 mm Hg, and (3) it is capable of dynamic three-dimensional oxygen imaging obtained every 2 to 3 minutes with 1- to 2-mm spatial resolution.

We have previously shown the feasibility of EPRI coupled with MRI operating at a common frequency of 300 MHz with 10-mT and 7-T magnetic fields, respectively (23). Sequential scans of EPRI and MRI are useful for a more complete examination of tumor hypoxia, blood perfusion, and energy metabolism. Recent developments in instrumentation and image

acquisition strategy made it possible to obtain three-dimensional pO_2 maps within 3 minutes, enabling noninvasive imaging of cycling hypoxia in tumors. Additionally, using a simple strategy of air-carbogen-air challenge during the imaging experiments with EPRI in a time window of 30 minutes provided the capability to spatially distinguish chronic hypoxic regions from cycling hypoxic regions in an animal model (22). Fig. 1A shows pO_2 images from an EPRI-based assessment of tumor oxygenation at 3, 18, and 27 minutes during an imaging time window of 30 minutes. The two regions of interest (ROI) 1 and 2 are identified as chronic or cycling hypoxic regions, respectively. Average pO_2 values in these regions are plotted at the various times when images were taken as shown in Fig. 1B. The lower curve corresponds to ROI 1, illustrating a region experiencing chronic hypoxia, whereas the upper curve represents ROI 2, a region typical of cycling hypoxia exhibiting ~20–mm Hg fluctuations of pO_2 over the time course. In the cycling hypoxic regions, periods of acute hypoxia followed by restoration to near normoxic conditions can be observed. Fig. 1C shows two parametric images constructed from the
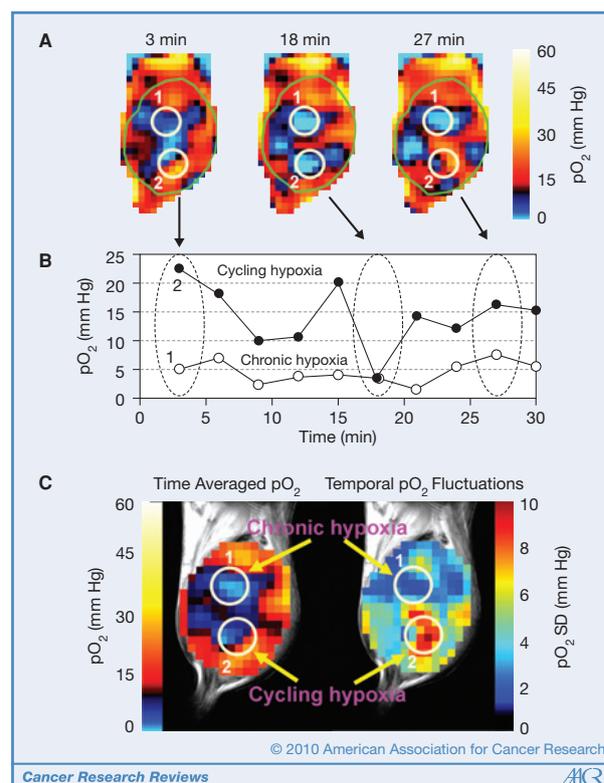

Figure 1. Noninvasive imaging of chronic and cycling tumor hypoxia in a mouse implanted with a SCCVII tumor. A, Three-dimensional–EPR oxygen images were obtained every 3 minutes during a 30-minute time window. Three representative images acquired at 3, 18, and 27 minutes are shown. Two ROIs were selected in the tumor (1 and 2), and pO_2 was assessed in the ROIs over 30 minutes. B, ROI 1 (open circles) indicates a chronically hypoxic region; ROI 2 (closed circles) represents a cycling hypoxic region showing temporal fluctuations in pO_2. C, Time-averaged pO_2 map (left) and standard deviation map of pO_2 (right) calculated from the 10 images taken in the 30-minute time window. For typical experimental conditions used for imaging, see refs. 22 and 23.

dynamic images shown in Figs. 1A and B. The image on the left in Fig. 1C is a time averaged pO_2 map from the tumor during the image time window of 30 minutes. The image on the right of Fig. 1C shows standard deviations of pO_2 map from the tumor from the 10 images taken in the 30-minute time window. The data displayed in this image contain information on the extent of temporal pO_2 fluctuations. In comparison to other pO_2 tissue-assessment technologies, EPRI clearly offers advantages. Nitroimadazole-based PET imaging and immunochemistry provide images similar to that shown in Fig. 1C (left), in which the temporal fluctuations are time averaged and a static assessment of tumor pO_2 is obtained. These techniques, therefore, do not provide information related to temporal fluctuations of pO_2. On the other hand, the images shown in Fig. 1A and B and the parametric image on the right of Fig. 1C contain spatial maps of fluctuations of pO_2. Polarographic oxygen electrodes or phosphorescence lifetime–optical imaging are capable of monitoring fluctuations in pO_2 in window-chamber models of tumors, with higher temporal resolutions in the order of seconds. However, the limited sampling volumes and invasive measures associated with the use of electrodes and tissue penetration of light with phosphorescence imaging may compromise assessment of deep-seated tumors.

EPRI-based approaches, whereas capable of monitoring pO_2 fluctuations in 2- to 3-minute temporal resolutions, can assess the tumor globally in three dimensions with a spatial resolution of ∼1 to 2 mm. Spontaneous near real-time cycling hypoxia can be measured directly without using experimentally enforced cycling hypoxia. Using EPRI, our recent study showed that the magnitude of fluctuations in pO_2 in spontaneous cycling hypoxia in tumors was associated with the maturity of tumor blood vessels (22). This result will require further study in different tumor types, but it shows that EPRI can effectively interrogate cycling hypoxia noninvasively and builds upon the wealth of information from research generated from prior reports (2, 8, 11–14, 16, 17, 19, 24, 25).

Future Directions

Recent data suggest that fluctuations in tumor pO_2 can impose resistance to radiotherapy by creating an aggressive tumor-cell phenotype with increased metastatic potential. Cycling hypoxia–mediated prosurvival pathways can also be initiated in tumor vascular endothelial cells, further contributing to treatment resistance (8, 17). How cycling tumor hypoxia impacts chemotherapy and molecularly targeted or immune-directed therapies is not known, but research to date suggests that it will be important in treatment response.

With the capability of noninvasive, temporal assessment of tumor pO_2 afforded by EPRI, it may be possible to assess HIF-1α induction and downstream genes regulated by HIF-1α in microregions of the tumor experiencing cycling and/or chronic hypoxia by the use of image-guided biopsies. Also, with inhibitors of HIF-1α now being developed for cancer therapy, EPRI can be useful in longitudinal monitoring of tumor pO_2 and the corresponding temporal fluctuations in response to treatment. Likewise, EPRI-based pO_2 assessment can readily be linked with other magnetic resonance technologies to further interrogate tumor physiology. For example, noninvasive modalities, such as magnetic resonance spectroscopy, which provide a biochemical assessment of microregions of a tumor, have already provided important information related to biochemical shifts and their relationship to treatment response (26). Further, magnetic resonance–based molecular imaging technologies can now assess the metabolic profile of tumor and/or normal tissue by following the metabolites of hyperpolarized pyruvate (27). These magnetic resonance–based images can readily be overlaid with EPRI-generated pO_2 maps to establish the link between tissue pO_2 and metabolism. EPRI pO_2 assessment, coupled with magnetic resonance–based metabolic images, could be integrated with treatment planning of intensity-modulated radiation therapy to deliver increased radiation doses to cycling and/or chronic hypoxia regions of the tumor. The concept of radiation "dose painting" of the tumor could then be based on the dynamic physiology in an individual's tumor, with the aim of improving treatment outcome. The treatment or diagnosis of diseases or disorders may also benefit from monitoring capabilities of EPRI-based pO_2 assessment including cardiovascular diseases, conditions secondary to diabetes, and inflammatory-related conditions.

Disclosure of Potential Conflicts of Interest

No potential conflicts of interest were disclosed.

References

1. Vaupel P, Mayer A. Hypoxia in cancer: significance and impact on clinical outcome. Cancer Metastasis Rev 2007;26:225–39.
2. Dewhirst MW. Relationships between cycling hypoxia, HIF-1, angiogenesis and oxidative stress. Radiat Res 2009;172:653–65.
3. Jain RK. Tumor angiogenesis and accessibility: role of vascular endothelial growth factor. Semin Oncol 2002;29:3–9.
4. Thomlinson RH, Gray LH. The histological structure of some human lung cancers and the possible implications for radiotherapy. Br J Cancer 1955;9:539–49.
5. Powers WE, Tolmach LJ. Demonstration of an anoxic component in a mouse tumor-cell population by in vivo assay of survival following irradiation. Radiology 1964;83:328–36.
6. Gatenby RA, Coia LR, Richter MP, Katz H, Moldofsky PJ, Engstrom P, et al. Oxygen tension in human tumors: in vivo mapping using CT-guided probes. Radiology 1985;156:211–4.
7. Dewhirst MW. Intermittent hypoxia furthers the rationale for hypoxia-inducible factor-1 targeting. Cancer Res 2007;67:854–5.
8. Martinive P, Defresne F, Bouzin C, Saliez J, Lair F, Grégoire V, et al. Preconditioning of the tumor vasculature and tumor cells by intermittent hypoxia: implications for anticancer therapies. Cancer Res 2006;66:11736–44.
9. Brown JM. Evidence for acutely hypoxic cells in mouse tumours, and a possible mechanism of reoxygenation. Br J Radiol 1979;52:650–6.

10. Yamaura H, Matsuzawa T. Tumor regrowth after irradiation; an experimental approach. Int J Radiat Biol Relat Stud Phys Chem Med 1979;35:201–19.
11. Chaplin DJ, Olive PL, Durand RE. Intermittent blood flow in a murine tumor: radiobiological effects. Cancer Res 1987;47:597–601.
12. Kimura H, Braun RD, Ong ET, Hsu R, Secomb TW, Papahadjopoulos D, et al. Fluctuations in red cell flux in tumor microvessels can lead to transient hypoxia and reoxygenation in tumor parenchyma. Cancer Res 1996;56:5522–8.
13. Cardenas-Navia LI, Mace D, Richardson RA, Wilson DF, Shan S, Dewhirst MW. The pervasive presence of fluctuating oxygenation in tumors. Cancer Res 2008;68:5812–9.
14. Dewhirst MW, Cao Y, Moeller B. Cycling hypoxia and free radicals regulate angiogenesis and radiotherapy response. Nat Rev Cancer 2008;8:425–37.
15. Cairns RA, Kalliomaki T, Hill RP. Acute (cyclic) hypoxia enhances spontaneous metastasis of KHT murine tumors. Cancer Res 2001;61:8903–8.
16. Moeller BJ, Cao Y, Li CY, Dewhirst MW. Radiation activates HIF-1 to regulate vascular radiosensitivity in tumors: role of reoxygenation, free radicals, and stress granules. Cancer Cell 2004;5:429–41.
17. Moeller BJ, Dreher MR, Rabbani ZN, Moeller BJ, Dreher MR, Rabbani ZN, et al. Pleiotropic effects of HIF-1 blockade on tumor radiosensitivity. Cancer Cell 2005;8:99–110.
18. Semenza GL. HIF-1 inhibitors for cancer therapy: from gene expression to drug discovery. Curr Pharm Des 2009;15:3839–43.
19. Baudelet C, Ansiaux R, Jordan BF, Havaux X, Macq B, Gallez B. Physiological noise in murine solid tumours using T2*-weighted gradient-echo imaging: a marker of tumour acute hypoxia? Phys Med Biol 2004;49:3389–411.
20. Lee N, Nehmeh S, Schoder H, Fury M, Chan K, Ling CC, et al. Prospective trial incorporating pre-/mid-treatment [18F]-misonidazole positron emission tomography for head-and-neck cancer patients undergoing concurrent chemoradiotherapy. Int J Radiat Oncol Biol Phys 2009;75:101–8.
21. Bennewith KL, Raleigh JA, Durand RE. Orally administered pimonidazole to label hypoxic tumor cells. Cancer Res 2002;62: 6827–30.
22. Yasui H, Matsumoto S, Devasahayam N, Munasinghe JP, Choudhuri R, Saito K, et al. Low-field magnetic resonance imaging to visualize chronic and cycling hypoxia in tumor-bearing mice. Cancer Res 2010; 70:6427–36.
23. Matsumoto S, Hyodo F, Subramanian S, Devasahayam N, Munasinghe J, Hyodo E, et al. Low-field paramagnetic resonance imaging of tumor oxygenation and glycolytic activity in mice. J Clin Invest 2008;118:1965–73.
24. Bennewith KL, Durand RE. Quantifying transient hypoxia in human tumor xenografts by flow cytometry. Cancer Res 2004;64:6183–9.
25. Lanzen J, Braun RD, Klitzman B, Brizel D, Secomb TW, Dewhirst MW. Direct demonstration of instabilities in oxygen concentrations within the extravascular compartment of an experimental tumor. Cancer Res 2006;66: 2219–23.
26. Kurhanewicz J, Swanson MG, Nelson SJ, Vigneron DB. Combined magnetic resonance imaging and spectroscopic imaging approach to molecular imaging of prostate cancer. J Magn Reson Imaging 2002;16:451–63.
27. Golman K, Zandt RI, Lerche M, Pehrson R, Ardenkjaer-Larsen JH. Metabolic imaging by hyperpolarized ^{13}C magnetic resonance imaging for in vivo tumor diagnosis. Cancer Res 2006;66:10855–60.

AACR American Association for Cancer Research

Imaging Cycling Tumor Hypoxia

Shingo Matsumoto, Hironobu Yasui, James B. Mitchell, et al.

Updated version	Access the most recent version of this article at: http://cancerres.aacrjournals.org/content/70/24/10019

Cited articles	This article cites 27 articles, 12 of which you can access for free at: http://cancerres.aacrjournals.org/content/70/24/10019.full#ref-list-1
Citing articles	This article has been cited by 10 HighWire-hosted articles. Access the articles at: http://cancerres.aacrjournals.org/content/70/24/10019.full#related-urls

E-mail alerts	Sign up to receive free email-alerts related to this article or journal.
Reprints and Subscriptions	To order reprints of this article or to subscribe to the journal, contact the AACR Publications Department at pubs@aacr.org.
Permissions	To request permission to re-use all or part of this article, use this link http://cancerres.aacrjournals.org/content/70/24/10019. Click on "Request Permissions" which will take you to the Copyright Clearance Center's (CCC) Rightslink site.